Intestinal CD103$^-$ dendritic cells migrate in lymph and prime effector T cells

Vuk Cerovic [a], Stephanie A. Houston [a], Charlotte L. Scott [a], Aude Aumeunier [a], Ulf Yrlid [b], Allan M. Mowat [a], Simon W.F. Milling [a]

[a] Institute for Infection, Immunity & Inflammation, College of Medical, Veterinary and Life Sciences, University of Glasgow, Glasgow, G12 8TA

[b] Department of Medical Microbiology and Immunology, University of Gothenburg, Gothenburg, Sweden

Correspondence: Vuk Cerovic

120 University Place

Glasgow, G12 8TA

Tel: +44 141 330 8141

Fax: +44 141 330 4297

Email: vuk.cerovic@glasgow.ac.uk

Running title: Immunogenic CD103$^-$ DCs in intestinal lymph

Abstract

Intestinal dendritic cells (DCs) continuously migrate through lymphatics to mesenteric lymph nodes (MLNs) where they initiate immunity or tolerance. Recent research has focused on populations of intestinal DCs expressing CD103. Here we demonstrate, for the first time, the presence of two distinct $CD103^-$ DC subsets in intestinal lymph. Similarly to $CD103^+$ DCs, these intestine-derived $CD103^-$ DCs are responsive to Flt3 and they efficiently prime and confer a gut-homing phenotype to naïve T cells. However, uniquely among intestinal DCs, $CD103^-$ $CD11b^+$ CX_3CR1^{int} lymph DCs (LDCs) induce the differentiation of both IFN-γ and IL-17-producing effector T cells, even in the absence of overt stimulation. Priming by $CD103^-$ $CD11b^+$ DCs represents a novel mechanism for the rapid generation of effector T cell responses in the gut. Therefore, these cells may prove to be valuable targets for the treatment of intestinal inflammation or in the development of effective oral vaccines.

Introduction

Dendritic cells (DCs) play a crucial role in maintaining the delicate balance between immunity and tolerance in the intestine. They migrate from the intestine, through lymphatics, to the mesenteric lymph nodes (MLNs) and prime the differentiation of naïve T lymphocytes into regulatory or effector cells. Understanding the functions of intestinal DCs is crucial for the development of oral vaccines and the treatment of inflammatory bowel disease. However, the precise identification of intestinal DCs is hindered by several factors. First, isolation of cells from the intestinal lamina propria (LP) necessitates mechanical and enzymatic disruption of tissue, which could alter the phenotype of isolated cells and may preferentially purify particular cell types [1]. Second, macrophages share many phenotypic characteristics with DCs, rendering surface marker expression alone inappropriate for unequivocal identification of DC populations. Importantly, intestinal macrophages do not migrate from the intestine to MLNs but remain in the LP, where they maintain and amplify the effector functions of T cells that migrate to the LP after being primed in the MLNs [2].

Recently, a subset of CD103 (integrin αE)-expressing $CD11c^+$ $MHCII^+$ LP cells (LPCs) has generated substantial interest. These $CD103^+$ LPCs are likely to represent *bona fide* DCs as they develop independently of M-CSF but expand in response to fms-like tyrosine kinase 3 ligand (Flt3L) and GM-CSF [3,4]. $CD103^+$ LP DCs express CCR7, and cells of a similar phenotype and function are present in the MLN. $CD103^+$ DCs from both the LP and the MLN induce differentiation of

naïve $CD4^+$ T cells into $FoxP3^+$ regulatory T cells [5,6], and drive responding T cells to express the gut-homing molecules CCR9 and $\alpha4\beta7$ [7].

Intestinal $CD103^+$ DCs are a heterogeneous population of cells and can be divided into two functionally distinct subsets: $CD11b^+$ $CD8\alpha^-$ and $CD11b^-$ $CD8\alpha^+$ [8,9]. The $CD8\alpha^+$ DCs represent a smaller subset of LP DCs, [3,9], and it is currently not clear whether they migrate in lymph or contribute to priming of naïve cells in the MLN [10].

In contrast to $CD103^+$DCs, $CD103^-$ DCs in the MLN are reported to have a more immunogenic phenotype in both the steady state [5] and in inflammation [11]. However, these $CD103^-$ MLN DCs are thought to originate from the blood and not from the intestine. Whether any $CD103^-$ DCs migrate from the LP to the MLN, and the role they may have in the induction of immune responses is currently a matter of controversy. The majority of $CD11c^+$ $MHCII^+$ $CD103^-$ LP cells express high levels of the chemokine receptor CX_3CR1 and, while they have been referred to as DCs [3,12], several lines of evidence have called this classification into question. Small intestinal (SI) LP CX_3CR1^{hi} $CD103^-$ cells express F4/80 [4], develop from monocytes in an M-CSF-dependent manner [3] and, crucially, are absent from afferent intestinal lymph [4]. On balance, it is likely that these $CD11c^+$ $MHCII^+$ $CX3CR1^{hi}$ cells represent intestinal macrophages [13].

While $CD103^-$ DCs are commonly found in peripheral tissues, it is not clear whether there are any *bona fide* $CD103^-$ DCs in the intestinal LP [14]. Intriguingly, a population of $MHCII^{hi}$ $CD11c^+$ cells expressing intermediate levels of CX_3CR1

appears distinct from CX_3CR1^{hi} macrophages. These cells are phenotypically heterogeneous and their exact functions remain unclear [4,15]. While the majority appear to have the phenotypic and functional properties characteristic of inflammatory macrophages [16], some may also share the FLt3-dependent ontogeny characteristic of DCs [4].

Here, we have used a novel approach to define intestinal DCs based on their ability to migrate in steady state intestinal lymph. We are therefore able to offer a definitive and comprehensive characterization of the phenotype and function of all intestine-derived, lymph-borne DCs. We show that, in addition to $CD103^+$ DCs, two distinct subsets of $CD103^-$ DCs constitutively migrate to the MLN. Furthermore, these $CD103^-$ DCs have Flt3 dependent ontogeny, are highly effective APCs, and can confer gut tropism to naïve T cells. Notably, in contrast to the $CD103^+$ migrating DCs, $CD103^-$ intestinal lymph DCs induce differentiation of IFN-γ and IL-17-producing effector T cells.

Results

Intestinal $CD103^+$ $CD8\alpha^+$, $CD103^+$ $CD11b^+$ and $CD103^-$ DCs migrate in lymph

A fundamental and defining feature of intestinal DCs is that they are able to migrate from the intestinal LP to the MLN through the intestinal lymphatics. We have adapted techniques previously used in rats [17] and mice [18,19] to isolate migrating intestinal DCs from murine thoracic duct lymph [20]. Unlike direct isolation of cells from afferent mouse intestinal lymphatics [4], thoracic duct cannulation yields sufficient numbers of cells for direct functional analyses of

purified DC subsets, and allows the collection of all MLN-bound DCs over a period of time. Very few, if any, DCs migrate from LNs via efferent lymphatics and the thoracic duct lymph of normal mice is largely devoid of $CD11c^+$ cells (Fig. 1 A). Six weeks after mesenteric lymphadenectomy (MLNx), the re-anastomosis of lymphatics allows "pseudo-afferent lymph" DCs to migrate from the intestine into the thoracic duct. Thoracic duct lymph from MLNx mice therefore contains a distinct population of $CD11c^+$ $MHCII^{hi}$ cells. (Fig. 1 A) which represent DCs migrating from the intestine to the MLN.

Our analysis of these intestinal lymph-borne DCs (LDCs) revealed a heterogeneous population of cells comprising at least three subsets, based on their expression of CD103, CD11b and CD8α (Fig. 1 B, C). As expected, the majority of LDCs expressed CD103; these could be split into two subsets: $CD103^+$ $CD11b^+$ $CD8\alpha^-$ (described as "$CD103^+$ $CD11b^+$" herein) and $CD103^+$ $CD11b^-$ $CD8\alpha^+$ ("$CD103^+$ $CD8\alpha^+$"). A smaller subset (14.2±4.2%) of migrating DCs did not express CD103 (Fig. 1 B, C). The three LDC subsets had distinct morphology. Whereas the $CD103^+$ $CD8\alpha^+$ LDCs displayed prominent 'spiny' dendrites, the $CD103^-$ and $CD103^+$ $CD11b^+$ LDCs had ruffled cell membranes, with shorter, more evenly-spaced protrusions (Fig. 1 D). The expression of CD172a (SIRPα) has been used to identify DC subsets in many mammalian species [20]. Here we observed uniformly high levels of CD172a expression on $CD103^+$ $CD11b^+$ LDCs and the majority of $CD103^-$ LDCs. In contrast, CD8α expression was confined to $CD103^+$ $CD11b^-$ $CD8\alpha^+$ LDCs. CD4 was expressed at similarly low levels on all three LDC subsets (Fig. 1 E). None of the LDCs expressed the pDC-specific

marker PDCA-1 (Fig. 1 E), confirming that pDCs do not migrate from rodent intestinal mucosa [21]. Interestingly, both the CD103$^-$ DCs and the CD103$^+$ CD11b$^+$ LDCs expressed low levels of F4/80 (Fig. 1 E). CD103$^+$ CD11b$^+$ LDCs also expressed low levels of Siglec F (Fig. 1 E), normally considered an eosinophil-specific marker [22]. However, their morphological characteristics and high levels of MHCII expression clearly mark LDCs as distinct from eosinophils. All three subsets of LDCs had a surface phenotype previously described as "semi-mature" [23], expressing high levels of surface MHCII but low levels of the costimulatory molecules CD40, CD80 and CD86 (Fig. 1 E).

CD103$^-$ LDCs efficiently prime CD4$^+$ and CD8$^+$ naïve T cells

Our analysis of lymph cells revealed the presence of a significant number of CD103$^-$ cells, which possess the phenotypic and migratory hallmarks of DCs. We next examined whether migratory CD103$^-$ cells possessed the other defining property of DCs, the ability to present antigen to naïve T cells. To do this, the three subsets of LDCs were sorted, pulsed with ovalbumin and co-cultured with CFSE labeled, naïve OVA-specific OT-1 (CD8$^+$) or OT-2 (CD4$^+$) TCR-transgenic T cells. As expected, CD103$^+$ LDCs could induce antigen-specific proliferation of T cells, although they differed markedly in their ability to present antigen to CD4$^+$ and CD8$^+$ T cells. Whereas CD103$^+$ CD11b$^+$ LDCs were more efficient than CD103$^+$ CD8α^+ LDCs at inducing proliferation of naïve CD4$^+$ T cells (Fig. 2 A, B), CD103$^+$ CD11b$^+$ LDCs were less effective than CD103$^+$ CD8α^+ LDCs at cross-presenting antigen to naïve CD8$^+$ T cells, especially at lower DC:T cell ratios (Fig. 2 C, D). Unexpectedly, the CD103$^-$ LDCs were better at inducing proliferation of

antigen-specific naïve CD4$^+$ T cells than either CD103$^+$ LDC subset, and were almost as efficient as CD8α^+ DCs at cross-presentation (Fig. 2 A-D). Therefore, their priming efficiency, as well as their migration pattern unambiguously identifies CD103$^-$ LDCs as *bona fide* DCs.

LDC subsets express ALDH and induce CCR9 expression on proliferating T cells

These data indicate that although CD103$^-$ LDCs comprise a relatively small proportion of migrating DCs, they may have a significant effect on the T cell response initiated in the MLN. We therefore explored their effects on the functional differentiation of naïve T cells *in vitro*. A hallmark of CD103$^+$ DCs from the LP and MLN is that they confer a gut-homing phenotype on interacting T cells, by virtue of their ability to metabolize dietary vitamin A into retinoic acid [7,24]. We examined LDCs for the activity of aldehyde dehydrogenase (ALDH), an enzyme required for retinoic acid generation, as measured by the fluorescence of the ALDEFLUOR substrate. All three subsets of intestinal LDCs exhibited high levels of ALDH activity, which was blocked by the specific inhibitor diethylaminobenzoaldehyde (DEAB) (Fig. 3 A, B). Moreover, when cultured with antigen-specific naïve CD8$^+$ T cells, all three LDC subsets were able to induce CCR9 expression on dividing T cells (Fig. 3 C). Therefore, the CD103$^-$ and CD103$^+$ intestinal LDC populations share the ability to confer gut tropism to differentiating T cells.

CD103$^-$ LDCs induce differentiation of IFN-γ and IL-17 producing T cells

To further investigate the functions of LDC subsets, we compared their ability to drive naïve $CD4^+$ and $CD8^+$ T cells to adopt an effector phenotype. As expected, both $CD4^+$ and $CD8^+$ T cells primed with either subset of $CD103^+$ LDCs produced little or no IFN-γ or IL-17 (Fig. 4 A, B) and low levels of IL-10 or IL-4 (data not shown). However, IFN-γ production from $CD8^+$ T cells was enhanced if the $CD103^+$ LDCs were first stimulated with bacterial lipoprotein (BLP), a TLR2 agonist (Fig. 4 B). BLP-stimulated $CD103^+$ LDCs also induced increased T cell proliferation, compared with unstimulated LDCs (data not shown).

In marked contrast to both $CD103^+$ LDC subsets, steady-state $CD103^-$ DCs induced both $CD4^+$ and $CD8^+$ T cells to produce high concentrations of IFN-γ, even in the absence of overt stimulation (Fig 4. A, B). Furthermore, $CD103^-$ LDCs were the only LDCs to induce IL-17 production by both OT-1 and OT-2 cells. Freshly isolated LDC subsets expressed very low mRNA levels of IL-12 and IL-23 subunits (data not shown), however, when cultured with an agonistic anti-CD40 antibody to mimic their interaction with cognate T cells, $CD103^-$ LDCs expressed at least 10-fold more mRNA for IL-12p40, IL-12p35 and IL-23p19, (Fig. 4 C). These data strongly suggest that expression of these cytokines confers the $CD103^-$ LDCs with their capacity to drive immunogenic T cell differentiation.

All LDC populations expressed very low levels of the IL-10 mRNA, even after culture with the anti-CD40 antibody (data now shown), in contrast to intestinal macrophage populations [25].

$CD103^-$ DCs comprise two distinct subsets in steady-state lymph and SI LP

Having identified CD103$^-$ LDCs as a novel migratory population of intestinal DCs, we sought to identify cells with a similar phenotype in the intestinal LP of $CX_3CR1^{gfp/+}$ mice [26]. Having first excluded macrophages based on their distinct (MHCII$^+$ F4/80^{hi} CX_3CR1^{hi}) phenotype (MΦ; Fig. 5A), we were able to identify DC subsets similar to those in lymph (Fig. 5 A, Supplementary Fig. 1). In both lymph and LP, CD103$^+$ DCs were CX_3CR1^- (P3, P4; Fig. 5 B). In contrast, the CD103$^-$ DC population in both sites was heterogeneous for CX_3CR1, and could be divided into CD103$^-$ CD11b$^-$ CX3CR1$^-$ (P1,) and CD103$^-$ CD11b$^+$ CX3CR1$^+$ (P2) populations (Figure 5 A, B). The majority of CD103$^-$ CD11b$^+$ DCs expressed CX_3CR1 at similar levels to the previously described CX_3CR1^{int} LP cell population and notably lower than the CX_3CR1^{hi} macrophages (Fig. 5 B) [4,15]. Importantly, all four LP DC populations, including both CD103$^-$ and both CD103$^+$ subsets, expressed similar levels of CCR7 mRNA, which was almost ten-fold higher than that found in LP macrophages (Fig. 5 C). All LPDC populations expressed very low levels of IL-10 mRNA (data not shown).

In order to gain a better understating of the biology of these phenotypically distinct, migrating DC subsets we next examined their anatomical origins in the intestine. To do this, we made use of RORγt$^{-/-}$ mice, which lack all secondary lymphoid tissues except the spleen and so, are devoid of Peyer's patches (PP) and isolated lymphoid follicles (ILFs) [27]. Despite previous reports that CD103$^+$ CD11b- CD8α$^+$ DCs mainly originate in the intestinal lymphoid tissues [10], they comprise a normal proportion of lymph DCs, and are present in normal numbers in the LP of RORγt$^{-/-}$ mice (Fig. 5 D). Similarly, the CD103$^+$ CD11b$^+$ and CD103$^-$ CD11b$^+$ populations were unchanged in RORγt$^{-/-}$ mice (Fig 5 D). In contrast, the CD103$^-$ CD11b$^-$ population was significantly reduced in the lymph and LP of

RORγt$^{-/-}$ mice (Fig. 5 D), indicating that the majority of these DCs may derive from organized intestinal lymphoid tissues, and not from the LP.

To ascertain whether both CD103^{-} subpopulations contribute to the priming of effector CD4^{+} T cells, they were sorted and incubated with ovalbumin and naïve OT-II T cells. Analysis of the supernatants revealed that both CD103^{-} LDC subsets induced IL-17 production from the OT-II T cells; however, the capacity to induce IFN-γ production was confined to the CD103^{-} CD11b^{+} subset of LDCs (Fig. 5 E). As before, neither of the CD103^{+} subsets could stimulate production of either IFN-γ or IL-17.

CD103^{-} DCs in the SI LP and intestinal lymph expand in response to Flt3L

To address the ontogeny of LDC subsets, mice were treated with recombinant Flt3L for 9 days prior to cannulation of the thoracic duct. This led to a significant increase in the frequency of all four DC subsets, both in the lymph (Fig. 6 A) and the SI LP (Fig. 6 B), but had no effect on F4/80^{hi} MHCI^{hi} LP macrophages (Fig. 6 B). These results support previous work showing the selective effect of Flt3L on SI LP CD103^{+} DCs and CD103^{-} DCs, but not the CX_3CR1^{hi} macrophages [4]. PCR analysis of growth factor receptor expression confirmed these findings by showing that all four subsets of LP DCs expressed hundred-fold more Flt3 mRNA than LP macrophages (Fig. 6 C). In contrast, LP DCs expressed at least ten-fold less CSF-1R mRNA than macrophages. Taken together, these experiments offer further evidence that the migrating CD103^{-} cells we identified represent genuine DCs, detectable in the steady-state lymph and LP.

Discussion

Intestinal DCs and macrophages share a number of phenotypic and functional features, which has made the elucidation of their respective roles in the initiation of peripheral tolerance and induction of immune responses challenging [1]. However, an important functional distinguishing feature of DCs is their ability to migrate in lymph to the draining MLNs. Here we sought to examine the phenotype and function of mouse intestinal DCs by direct examination of $CD11c^+$ $MHCII^+$ cells in intestinal pseudo-afferent lymph. Our studies revealed the existence of three distinct subset of migrating DCs: $CD103^+$ $CD11b^+$, $CD103^+$ $CD8\alpha^+$ and $CD103^-$. These findings are novel and surprising for a number of reasons. First, while $CD103^+$ $CD11b^+$ DCs make up the majority of $CD103^+$ LP DCs in the small intestine and their migration to the MLN has been well documented [3,8,10], the fate of $CD103^+$ $CD8\alpha^+$ DCs is less clear. Although a distinct subset of $CD103^+$ LP DCs has recently been shown to express $CD8\alpha$ [9], and fewer $CD8\alpha^+$ DCs are found in the MLNs of $CCR7^{-/-}$ mice [28], $CD8\alpha^+$ DC are generally thought to reside mostly within secondary lymphoid organs and not to migrate in lymph. [10]. To our knowledge, the data shown here represent the first definitive evidence that $CD103^+$ $CD8\alpha^+$ DCs constitutively migrate from the intestine to the MLN.

Moreover, the $CD103^+$ $CD11b^-$ $CD8\alpha^+$ DCs were present in normal numbers in the lymph and LP of $ROR\gamma t^{-/-}$ mice, which lack PPs and ILFs, indicating that the majority of these DCs derive from the LP of the conventional villus mucosa. The $CD8\alpha^+$ LDCs were especially effective at cross-presentation to $CD8^+$ T cells, and far less effective at priming $CD4^+$ T cells than $CD8\alpha^-$ LDCs. Similar specialization

of CD8α$^+$ and CD8α$^-$ DCs has been described in other tissues including the SI LP [8,9].

Our second important finding was of a significant number of CD103$^-$ DCs in intestinal lymph, suggesting that CD103 cannot be used as a de-facto marker of migratory intestinal DCs in MLN, as has become convention [4,5,9,24]. While CD103$^-$ cells make up the majority of CD11c^{hi} MHCII$^+$ cells in the LP, the only previous study of afferent intestinal lymph detected exiguous numbers of these cells [4] and hence they are generally considered to be sessile intestinal macrophages [13]. Despite sharing some phenotypic characteristics of macrophages, including the expression of the fractalkine receptor CX_3CR1, CD103$^-$ LDCs are *bona fide* DCs; they are highly efficient at priming naïve T cells and continuously migrate from tissue to draining LNs. Crucially, cells with the same surface phenotype are present in the SI LP and express high levels of CCR7 mRNA (Figure 5).

Furthermore, these intestine-derived CD103$^-$ DCs share important functional and phenotypic properties with CD103$^+$ LDCs. All LDC subsets were able to present antigen to naïve T cells and induce CCR9 expression of dividing T cells. Importantly, CD103$^-$ DCs comprise two distinct subsets, separated by their expression of CD11b and CX_3CR1, and by their distinct anatomical origins. CD103$^-$ CD11b$^+$ CX3CR1^{int} DCs are present in normal numbers in RORγt$^{-/-}$ mice, indicating that they mainly reside in the villus LP. Conversely, the CD103$^-$ CD11b$^-$ CX3CR1$^-$ DCs are absent from the intestine of RORγt$^{-/-}$ mice and are therefore likely to mainly derive from the organized intestinal lymphoid tissues such as the PPs and ILFs.

Crucially, cells of a similar phenotype to all four LDC subsets were detectable in the SI LP of steady-state mice and were expanded to a similar extent in the LP and intestinal lymph by treatment with Flt3L. Additionally, all four LP DC subsets expressed Flt3 mRNA at a markedly higher level than intestinal macrophages. Therefore, all the LPDCs and LDCs we describe here are responsive to Flt3L, while LP Mϕs are not. Taken together with the fact that the LPDC populations all express 100-fold higher levels of Flt3 mRNA than LP Mϕs, these data further indicate that LDC and LPDC populations are distinct from LP Mϕs. Interestingly, the Flt3L-induced expansion of the LP and lymph $CD103^+$ $CD11b^+$ compartment was much less pronounced than either the $CD103^-$ or $CD8\alpha^+$ DCs. Thus the development of $CD103^+$ $CD11b^+$ intestinal DCs may require an additional growth factor, independent of Flt3 signaling, as previously suggested [3].

Interestingly, $CD103^+$ and $CD103^-$ LDCs had distinct effects on the differentiation of primed T lymphocytes. While both $CD103^+$ LDCs subsets induced naïve T cell proliferation, they only induced IFN-γ production in proliferating T cells after activation by a TLR ligand. These observations are consistent with previous reports, demonstrating that steady state $CD103^+$ DCs in the SI LP [8,9,29] and rat intestinal lymph [30] induce inflammatory cytokine production following TLR activation. Conversely, $CD103^-$ DCs expressed higher levels of IL-12 and IL-23 mRNA and induced IFN-γ and IL-17 production from proliferating T cells even in the absence of TLR stimulation. Coupled with their ability to confer gut-tropism to effector cells, priming by $CD103^-$ intestinal DCs is likely to represent an important mechanism for the initiation of gut-specific adaptive immune responses. In addition, IL-23 and IL-17 have a well-defined role in the induction of inflammatory responses in the gut [31,32]. Further functional analysis revealed

that while both populations of CD103$^-$ DCs were able to induce IL-17 production from T cells in the steady state, only the CD103$^-$ CD11b$^+$ CX3CR1^{int} DCs were able to induce IFNγ. Interestingly, whereas most data on steady-state intestinal DCs indicate that their function is tolerogenic, a role for intestinal CD11c$^+$ MHCII$^+$ CD11b$^+$ LP DCs in the induction of IFN-γ and IL-17 has previously been proposed [33]. The authors described a heterogeneous population that was largely CD103$^-$ CD11b$^+$ and is likely to have contained at least some macrophages. Here, we have combined detailed phenotyping of intestinal populations with analysis of lymph cells, revealing *bona fide* IFN-γ and IL-17-inducing DCs within this CD11c$^+$ CD11b$^+$ population.

Recently, a small population of colonic CD11c$^+$ CX3CR1^{int} cells has been identified, which share some phenotypic characteristics with our LDCs. These colonic cells increase in number after induction of experimental colitis [25]. It is therefore possible that immunogenic DCs are maintained in low numbers in intestinal tissues in the steady state, and are rapidly recruited upon the disruption of intestinal homeostasis.

Here we offer a definitive characterization of all migrating intestinal DCs and describe, for the first time, a specialized intestinal CD103$^-$ DC subset capable of inducing IFN-γ and IL-17 production from naïve T cells. Importantly, these CD103$^-$ DCs confer gut-tropism to differentiating T cells, and may therefore represent an important mechanism for the induction of immune responses in the intestinal mucosa. Despite the presence of these immunostimulatory CD103$^-$ DCs in the steady state, the balance of the intestinal immune system favors the maintenance of tolerance. This may reflect the fact that CD103$^-$ DCs are present in much lower numbers than the tolerogenic CD103$^+$ DCs. We suggest that the

balance between $CD103^-$ DCs, $CD103^+$ DCs and intestinal macrophages is critical for maintaining intestinal immune homeostasis. Therefore, investigating how the functions of $CD103^-$ and $CD103^+$ LDCs change in response to pathogenic or inflammatory stimuli will provide essential insights into the development of intestinal immunopathology and the initiation of immune responses against intestinal pathogens. Finally, targeting $CD103^-$ intestinal DCs may prove to be an important strategy for enhancing immune responses to orally-administered vaccines.

MATERIALS AND METHODS

Animals

C57/Bl6 mice were purchased from Harlan and maintained in individually ventilated cages. OT-1, OT-2, $ROR\gamma t^{-/-}$ (originally from Prof. Dan Littman) and $CX_3CR1^{GFP/+}$ mice (originally from Dr. Steffen Jung) were bred and maintained under specific pathogen free (SPF) conditions at Central Research Facility, Glasgow. All procedures were approved by the local ethical committee and conducted under licenses issued by the UK Home Office.

Surgical procedures

Mesenteric lymphadenectomy and thoracic duct cannulation procedures were modified from established protocols [17]. Mesenteric lymphadenectomy was performed on six-week old male mice by laparotomy and blunt dissection. Six weeks later, mice were fed 0.2ml olive oil to visualize the lymphatics and the thoracic lymph duct was cannulated by the insertion of a polyurethane cannula (2Fr, Linton Instrumentation, Diss, UK). Lymph was collected in PBS with 20

U/ml of heparin sodium (Wockhardt UK, Wrexham, UK), on ice, for up to 16h. During surgical procedures the animals were maintained under inhalation anesthesia with Isoflurane (Abbot Animal Health, Abbott Park, IL).

Reagents

Cells were cultured in RPMI 1640, supplemented with 100 U/ml penicillin, 100 μg/ml streptomycin, 2mM L-glutamine, 5% FCS (all from Invitrogen, Paisley, UK), and 50μM 2-mercaptoethanol (2-ME; Sigma-Aldrich, St Louis, MO). BLP (Pam3CSK4; Invivogen, San Diego, CA) was used at 2.5μg/ml to activate the DCs in culture. Recombinant human Flt3L (Amgen, Seattle, WA) was injected intraperitoneally at 10μg per mouse per day for nine days.

Antibodies

Fluorochrome- or biotin- conjugated monoclonal antibodies to mouse antigens CD11b (M1/70), CD11c (HL3), CD40 (3/23), CD45 (RA3-6B2), CD80 (16-10A1), CD86 (GL1), CD172a (P84), Integrin β7 (FIB27), and Siglec F (E50/2440) were from BD Biosciences (Oxford, UK). The monoclonal Abs to mouse antigens CD4 (RM4-5), CD8α (53-6.7), CD19 (6D5), CD103 (2E7), CD44 (IM7), CD62L (MEL-14) were from Biolegend (San Diego, CA). The I-A/I-E MHCII (M5/114.15.2) and F4/80 (BM8) Abs were purchased from eBioscience (San Diego, CA). The PDCA-1 and the agonistic anti-CD40 antibody (FGK45.5) were purchased from Miltenyi Biotec (Auburn, CA). Streptavidin Qdot-605 was purchased from Invitrogen. The Viaprobe dead cell exclusion dye (7AAD) and mouse isotype control antibodies, conjugated to appropriate fluorochromes, were purchased from BD Biosciences. CCR9 staining was detected with the 7E7 antibody (gift from Oliver Pabst, MHH Hanover), and a secondary goat anti-rat Ig antibody (BD Biosciences). Staining

for ALDH was performed using the ALDEFLUOR kit (StemCell Technologies, Grenoble, France) according to manufacturer's instructions.

Cell isolation

Thoracic duct leukocytes were collected on ice in PBS with 20 U/ml Heparin, passed through a 40 μm cell strainer (BD Biosciences), and RBCs lysed with ACK lysis buffer (Sigma-Aldrich). Cells were stained and analyzed by flow cytometry or sorted by FACS using the FACSAria cell sorter (BD Biosciences).

Small intestines were flushed with HBSS 2% FCS and the Peyer's patches excised. The intestines were opened longitudinally and cut into 0.5cm segments, which were incubated twice in HBSS with 2mM EDTA at 37°C while shaking for twenty minutes. Supernatants were discarded and the tissue digested with 1mg/ml of collagenase VIII (Sigma-Aldrich) at 37°C with shaking for 15 minutes. Cells were passed through a 40 μm cell strainer and stained for flow cytometry.

Flow cytometry

Cell surface staining was performed in PBS with 2% FCS and 10 mM EDTA for 30 min on ice. Where biotin-conjugated antibody was used, cells were further stained with a streptavidin-fluorochrome conjugate for 15 min. Samples were acquired on LSRII (BD Biosciences) or MACSQuant (Miltenyi Biotec) flow cytometers or sorted and analyzed by the FACSAria cell sorter (BD Biosciences). Acquired data was analyzed using FlowJo software (version 9.3.1; Tree Star, Inc, Ashland, OR).

Microscopy

Cells were centrifuged (300rpm, 5 min) onto poly-L-Lysine coated slides (VWR International, Radnor, PA) and stained using the Rapid Romanowsky staining kit (Thermo Fisher Scientific, Waltham, MA). Images were obtained using a light

microscope at 40x magnification and were analyzed and archived using cell^B software (Olympus, Tokyo, Japan).

Proliferation assay

Sorted LDCs were pulsed with 2mg/ml of ovalbumin (Worthington, Lakewood, NJ) for 2h at 37°C and then extensively washed. They were cultured at varying ratios with 10^5 CFSE-labeled naïve OT-1 or OT-2 cells at 37°C for three days. CFSE dilution was assessed by flow cytometry.

Cytokine detection

DCs and T cells were co-cultured for three days, then incubated for 4h with phorbol 12-myristate 13-acetate (PMA) and Ionomycin (both from Sigma-Aldrich) and the supernatants harvested. Concentrations of IFN-γ, IL-17, IL-10 and IL-4 were assessed by the Milliplex cytokine bead assay (Millipore, Billerica, MA) according to manufacturer's instructions. Minimum detectable concentrations for all cytokines were less than 5 pg/ml.

RNA extraction

RNA was extracted using the MicroRNA kit (Qiagen, Venlo, Netherlands) according to manufacturer's instructions. Contaminating genomic DNA was removed using the DNA-free kit (Qiagen). RNA was reverse transcribed using Superscript First Strand kit (Invitrogen).

Real-time quantitative PCR

cDNA was examined for the frequency of different transcripts using quantitative real-time PCR. IL-12 and IL-23 subunits were analyzed using the Taqman probe system. All qPCR Taqman reactions were performed in 20μl volumes using colorless master mix (Promega, Fitchburg, WI) and primer/probe sets designed and validated by Applied Biosystems (Foster City, CA; Mm00518984_m1,

Mm00434165_m1, Mm00434174_m1, Mm00446968_m1). Fluorescence levels were detected and analyzed using the 7900HT Fast system (Applied Biosystems). All other qPCR reactions were performed using the Brilliant III Ultra Fast SYBR qPCR master mix (Agilent Technologies, Santa Clara, CA). Primers used were HPRT: forward GCTGACCTGCTGGATTACATTAA, reverse TGATCATTACAGTAGCTCTTCAGTCTGA; CCR7: forward ATTGCTGCTGAGGGAAGAG, reverse ACTTTTGGCTGTCGTTTTGG; CSF-1R: forward GCATACAGCATTACAACTGGACCTACC, reverse CAGGACATCAGAGCCATTCACAG; Flt3: forward GGTTTAAAGCGTACCCACGA, reverse GAACTGGGCGTCATCATTTT. Relative quantification was determined using the ΔΔCt method and normalized to expression of the housekeeping gene HPRT.

Statistical analysis

For comparison of means between two groups, the data were analyzed using a student's t-test unless otherwise indicated. For comparisons involving more than two data sets, an analysis of variance (ANOVA) was used. P-values less than 0.05 were considered significant and Bonferroni post-test was performed on the data sets. All statistical analysis was performed using GraphPad Prism and Microsoft Excel.

Acknowledgements

We thank Drs. Gordon MacPherson and Andrew MacDonald for critical reading of the manuscript, Dr. William Agace for providing the $CX_3CR1^{GFP/+}$ animals and Prof. Peter Lane for the $ROR\gamma t^{-/-}$ mice. The authors acknowledge Laura Ford for

technical assistance and the University of Glasgow Flow Cytometry Core Facility for assistance with cell sorting. VC was funded by a Medical Research Council award to SWFM; AA, CLS and AMM were funded by the Wellcome Trust. SAH was supported by a Capacity Building Award in Integrative Mammalian Biology funded by the BBSRC, BPS, KTN, MRC and SFC, AstraZeneca, GlaxoSmithKline and Pfizer.

Disclosure

The authors have no conflicting financial interests.

References

1. Pabst, O. & Bernhardt, G. The puzzle of intestinal lamina propria dendritic cells and macrophages. *European journal of immunology* **40**, 2107-2111 (2010).
2. Hadis, U.*, et al.* Intestinal Tolerance Requires Gut Homing and Expansion of FoxP3(+) Regulatory T Cells in the Lamina Propria. *Immunity* **34**, 237-246 (2011).
3. Bogunovic, M.*, et al.* Origin of the lamina propria dendritic cell network. *Immunity* **31**, 513-525 (2009).
4. Schulz, O.*, et al.* Intestinal CD103+, but not CX3CR1+, antigen sampling cells migrate in lymph and serve classical dendritic cell functions. *The Journal of experimental medicine* **206**, 3101-3114 (2009).
5. Coombes, J.L.*, et al.* A functionally specialized population of mucosal CD103+ DCs induces Foxp3+ regulatory T cells via a TGF-{beta} and retinoic acid dependent mechanism. *The Journal of experimental medicine* **204**, 1757-1764 (2007).
6. Sun, C.M.*, et al.* Small intestine lamina propria dendritic cells promote de novo generation of Foxp3 T reg cells via retinoic acid. *The Journal of experimental medicine* **204**, 1775-1785 (2007).
7. Johansson-Lindbom, B.*, et al.* Functional specialization of gut CD103+ dendritic cells in the regulation of tissue-selective T cell homing. *The Journal of experimental medicine* **202**, 1063-1073 (2005).
8. Uematsu, S.*, et al.* Regulation of humoral and cellular gut immunity by lamina propria dendritic cells expressing Toll-like receptor 5. *Nat Immunol* **9**, 769-776 (2008).
9. Fujimoto, K.*, et al.* A New Subset of CD103+CD8{alpha}+ Dendritic Cells in the Small Intestine Expresses TLR3, TLR7, and TLR9 and Induces Th1 Response and CTL Activity. *J Immunol* (2011).
10. Jakubzick, C.*, et al.* Lymph-migrating, tissue-derived dendritic cells are minor constituents within steady-state lymph nodes. *The Journal of experimental medicine* **205**, 2839-2850 (2008).
11. Siddiqui, K.R., Laffont, S. & Powrie, F. E-cadherin marks a subset of inflammatory dendritic cells that promote T cell-mediated colitis. *Immunity* **32**, 557-567 (2010).
12. Niess, J.H.*, et al.* CX3CR1-mediated dendritic cell access to the intestinal lumen and bacterial clearance. *Science* **307**, 254-258 (2005).
13. Persson, E.K., Jaensson, E. & Agace, W.W. The diverse ontogeny and function of murine small intestinal dendritic cell/macrophage subsets. *Immunobiology* **215**, 692-697 (2010).
14. Ginhoux, F.*, et al.* The origin and development of nonlymphoid tissue CD103+ DCs. *The Journal of experimental medicine* **206**, 3115-3130 (2009).
15. Varol, C.*, et al.* Intestinal lamina propria dendritic cell subsets have different origin and functions. *Immunity* **31**, 502-512 (2009).

16. Weber, B., Saurer, L., Schenk, M., Dickgreber, N. & Mueller, C. CX3CR1 defines functionally distinct intestinal mononuclear phagocyte subsets which maintain their respective functions during homeostatic and inflammatory conditions. *European journal of immunology* **41**, 773-779 (2011).
17. Milling, S.W., Jenkins, C. & MacPherson, G. Collection of lymph-borne dendritic cells in the rat. *Nat Protoc* **1**, 2263-2270 (2006).
18. Rhodes, J.M. Isolation of large mononuclear Ia-positive veiled cells from the mouse thoracic duct. *Journal of immunological methods* **85**, 383-392 (1985).
19. Ionac, M. One technique, two approaches, and results: thoracic duct cannulation in small laboratory animals. *Microsurgery* **23**, 239-245 (2003).
20. Milling, S., Yrlid, U., Cerovic, V. & MacPherson, G. Subsets of migrating intestinal dendritic cells. *Immunol Rev* **234**, 259-267 (2010).
21. Yrlid, U.*, et al.* Plasmacytoid dendritic cells do not migrate in intestinal or hepatic lymph. *J Immunol* **177**, 6115-6121 (2006).
22. Zhang, J.Q., Biedermann, B., Nitschke, L. & Crocker, P.R. The murine inhibitory receptor mSiglec-E is expressed broadly on cells of the innate immune system whereas mSiglec-F is restricted to eosinophils. *European journal of immunology* **34**, 1175-1184 (2004).
23. Lutz, M.B. & Schuler, G. Immature, semi-mature and fully mature dendritic cells: which signals induce tolerance or immunity? *Trends in immunology* **23**, 445-449 (2002).
24. Jaensson, E.*, et al.* Small intestinal CD103+ dendritic cells display unique functional properties that are conserved between mice and humans. *The Journal of experimental medicine* **205**, 2139-2149 (2008).
25. Rivollier, A., He, J., Kole, A., Valatas, V. & Kelsall, B.L. Inflammation switches the differentiation program of Ly6Chi monocytes from antiinflammatory macrophages to inflammatory dendritic cells in the colon. *The Journal of experimental medicine* **209**, 139-155 (2012).
26. Jung, S.*, et al.* Analysis of fractalkine receptor CX(3)CR1 function by targeted deletion and green fluorescent protein reporter gene insertion. *Molecular and cellular biology* **20**, 4106-4114 (2000).
27. Sun, Z.*, et al.* Requirement for RORgamma in thymocyte survival and lymphoid organ development. *Science* **288**, 2369-2373 (2000).
28. Jang, M.H.*, et al.* CCR7 is critically important for migration of dendritic cells in intestinal lamina propria to mesenteric lymph nodes. *J Immunol* **176**, 803-810 (2006).
29. Kinnebrew, M.A.*, et al.* Interleukin 23 Production by Intestinal CD103(+)CD11b(+) Dendritic Cells in Response to Bacterial Flagellin Enhances Mucosal Innate Immune Defense. *Immunity* **36**, 276-287 (2012).
30. Cerovic, V.*, et al.* Hyporesponsiveness of Intestinal Dendritic Cells to TLR Stimulation Is Limited to TLR4. *J Immunol* **182**, 2405-2415 (2009).
31. Maloy, K.J. & Powrie, F. Intestinal homeostasis and its breakdown in inflammatory bowel disease. *Nature* **474**, 298-306 (2011).
32. Uhlig, H.H.*, et al.* Differential activity of IL-12 and IL-23 in mucosal and systemic innate immune pathology. *Immunity* **25**, 309-318 (2006).

33. Denning, T.L., Wang, Y.C., Patel, S.R., Williams, I.R. & Pulendran, B. Lamina propria macrophages and dendritic cells differentially induce regulatory and interleukin 17-producing T cell responses. *Nat Immunol* **8**, 1086-1094 (2007).

Figure legends

Figure 1. Phenotype of intestinal lymph-borne mouse DCs. Thoracic duct cannulation was performed on 12-week old MLNx C57Bl6 mice and lymph collected for 16 hours, on ice. Lymph cells were washed and stained for multi-color flow cytometry. a) Dendritic cells, identified as $CD11c^+$ $MHCII^{hi}$, were absent in efferent lymph of untreated mice but present in pseudo-afferent lymph of MLNx mice. Numbers show the percentage of live cells. b) $CD11c^+$ $MHCII^{hi}$ cells can be divided into three subsets based on the expression of CD103, CD11b and CD8α. c) Percentage of the three subsets of LDCs within the $CD11c^+$ $MHCII^{hi}$ population. Each dot represents an independent experiment. d) The three LDC subsets were gated as in b) and sorted by FACS. The sorted cells were spun onto slides and stained to observe the morphology. The scale bar represents 50μm. e) Expression of a range of phenotypic markers, MHCII and costimulatory molecules CD40, CD80 and CD86 on LDC subsets. The histograms show the expression of the indicated marker on $CD103^-$ (green), $CD103^+$ $CD11b^+$ (red) and $CD103^+$ $CD8\alpha^+$ (blue) cells. The filled histogram represents the appropriate isotype control gated on total $CD11c^+$ $MHCII^{hi}$ cells. Results in d) and e) are representative of three independent experiments.

Figure 2. Subsets of LDCs prime and cross-prime naïve T cells with different efficiencies. $CD103^-$, $CD103^+$ $CD11b^+$ and $CD103^+$ $CD8\alpha^+$ LDCs were sorted by

FACS and incubated for 2h with 2mg/ml of ovalbumin protein. DCs were extensively washed and plated out at a range of dilutions with 10^5 CFSE-labeled (a and b) sorted $CD4^+$ $CD62L^+$ OT-2 cells or (c and d) $CD8^+$ $CD62L^+$ OT-1 cells for three days. Proliferation was assessed by CFSE dilution. a) and c) Data are presented as mean ± SD and are pooled from 4 independent experiments. Asterisks denote statistical significance (* $p< 0.05$, ** $p<0.01$) b) and d) examples of CFSE dilution induced by the three LDC subsets at 12,500 DCs per well.

Figure 3. LDC subsets show ALDH activity and can induce CCR9 expression on responding T cells. a) Lymph cells were incubated with the fluorescent ALDH substrate ALDEFLUOR and stained for flow cytometry. The three LDC subsets were gated as in Fig. 1, and lymph B cells ($CD19^+$ $MHCII^+$) used as a negative control. Histograms represent green fluorescence in the presence (grey filled histograms) or absence (white histograms) of the ALDH inhibitor DEAB. b) Mean fluorescence intensity of ALDEFLUOR in the three subsets of LDCs in the presence or absence of DEAB. Each dot represents an individual biological replicate. c) LDC subsets were sorted by FACS, incubated for 2h with 2mg/ml of ovalbumin protein, washed and plated out at 1:8 DC:T cell ratio with 10^5 CFSE-labeled sorted naïve $CD8^+$ OT-1 cells and cultured for three days. Proliferating T cells were analyzed for the expression of CCR9. All data are representative of 3 independent experiments.

Figure 4. CD103- LDCs induce the differentiation of IFN-γ and IL-17 producing T cells. LDC subsets were sorted and cultured for 2h with 2mg/ml of ovalbumin protein with or without the addition of 2.5 μg/ml of BLP. DCs were

then washed and co-cultured for three days at 1:8 DC:T cell ratio with 10^5 sorted naïve $CD62L^+$ OT-2 (a) or OT-1 (b) T cells. IFN-γ and IL-17 production were assessed by luminex. Data are presented as mean of three replicates. c) Expression of mRNA encoding IL-12p35, IL-12p40 and IL-23p19 in LDC subsets following overnight culture with 10μg/ml of anti-CD40 mAb was assessed by qPCR. Data were normalized to the expression of the housekeeping gene HPRT and presented as relative expression (AU= arbitrary units). All data are representative of 2 independent experiments.

Figure 5. Functionally and anatomically distinct subpopulations of $CD103^-$ DCs in intestinal LP and lymph. Small intestine LP cells were isolated as described in the methods and the lymph collected by thoracic duct cannulation of MLNx mice. Cells were analyzed by flow cytometry. A) LP cells from $CX_3CR1^{gfp/+}$ mice were isolated and analyzed by flow cytometry. Single cells were gated based on physical characteristics and live leukocytes identified as $7AAD^-$ $CD45^+$ cells (not shown). Macrophages were identified as $F4/80^+$ cells with high expression of MHCII (MΦ). Macrophages universally express CD11b and high levels of CX_3CR1-GFP. Amongst $F4/80^{lo}$ cells, $MHCII^{hi}$ $CD11c^+$ cells were gated as DCs, and further split into $CD103^-$ $CD11b^-$ (P1), $CD103^-$ $CD11b^+$ (P2) $CD103^+$ $CD11b^+$ (P3) and $CD103^+$ $CD11b^-$ (P4) subsets. B) Live, $CD45^+$ cells were further gated as $CD11c^+$, $MHCII^+$, $F4/80^{lo}$ and subpopulations analyzed for CD103 and CD11b expression. $CD103^-$ $CD11b^-$ (orange), $CD103^-$ $CD11b^+$ (green), $CD103^+$ $CD11b^+$ (red) and $CD103^+$ $CD11b^-$ (blue) cells were analyzed for level of GFP expression in the small intestine LP (top) and pseudo-afferent intestinal lymph (bottom). The black histogram denotes CX_3CR1 GFP expression in $F4/80^{hi}$

MHCII$^+$ macrophages in the SI LP. C) Intestinal LP cells were gated as in A) and purified by FACS. qPCR was used to determine the relative expression of CCR7 mRNA, normalized to the housekeeping gene HPRT. D) SI LP and pseudo-afferent lymph cells from RORγt$^{-/-}$ mice were isolated and analyzed by flow cytometry. Representative plots show lymph (left) or SI LP DCs (right) gated as in A) from wild-type or RORγt$^{-/-}$ mice. Graphs represent the percentage of each subset among LDCs (left) or the total number of cells for each DC subset in the SI LP (right). Data are represented as mean ± SD and are from 2 independent experiments. Asterisks denote statistical significance (* $p< 0.05$). E) Four LDC subsets were sorted and cultured for 2h with 2mg/ml of ovalbumin protein. DCs were then washed and co-cultured for three days at 1:8 DC:T cell ratio with 10^5 sorted naïve CD62L$^+$ OT-2 T cells. IFN-γ and IL-17 concentrations in the supernatants were assessed by luminex. Data are representative of three (A, B) or two (C, E) independent experiments.

Figure 6. Shared ontogeny of CD103$^-$ and CD103$^+$ intestinal DCs. MLNx A) or normal B) C57Bl6 mice were injected i.p. with 10µg of recombinant hFlt3L daily for nine days. A) Mice were cannulated at day 9 and the lymph cells analyzed by flow cytometry. Representative plots show the proportion of LDC cells (left) and the proportion of each subset within the DC gate with or without Flt3L treatment. Graphs show the proportion of total LDCs (left) and the three LDC subsets (right) among live cells in untreated or Flt3L-treated mouse lymph. B) LP cells were analyzed by flow cytometry and the subsets were gated as in Fig 5a. Plots were gated on live CD45$^+$ CD11c$^+$ MHCII$^+$ F4/80$^-$ cells and show the proportion of each DC subset. The graphs represent the proportion of each

subset within the $CD45^+$ $7AAD^-$ compartment (left) or total number of cells (right). Each point in A) and B) represents a biological replicate. Results were analyzed by Mann-Whitney U test; asterisks denote statistical significance (* $p< 0.05$, ** $p<0.01$). C) SI LP Macrophages and four DC subsets were gated as in figure 5A and sorted by FACS. qPCR was used to assess the levels of FLt3 and CSF-1R mRNA expression, normalized to the expression of the housekeeping gene HPRT. The graphs are representative of two independent experiments.

Supplementary figure 1: **Phenotype of DC subsets present in lymph and LP.** DCs from pseudo-afferent lymph or small intestinal LP were gated as described in figure 5. Histograms show the expression of indicated markers, or staining with isotype control antibodies.

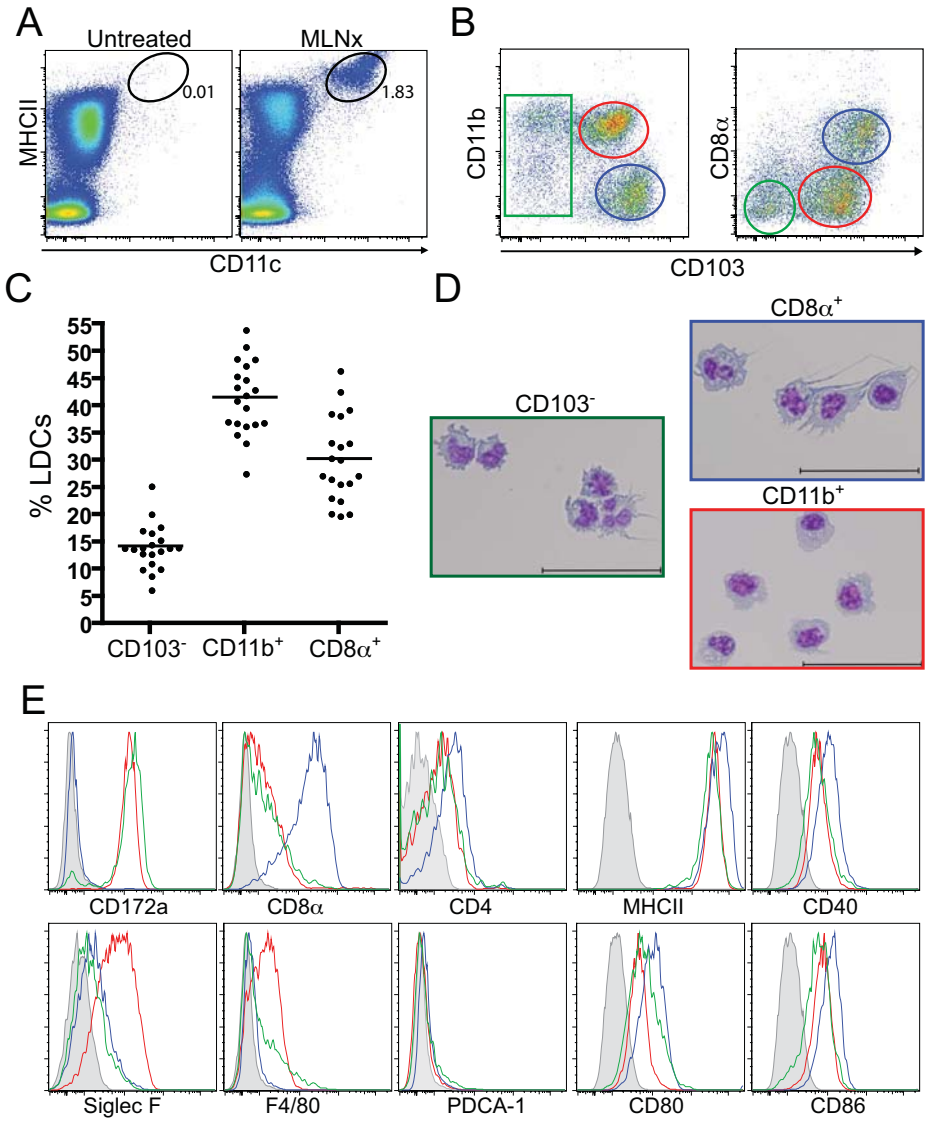
A
Untreated
MLNx
0.01
1.83
MHCII
CD11c
B
CD11b
CD8α
CD103
C
% LDCs
55
50
45
40
35
30
25
20
15
10
5
0
CD103-
CD11b+
CD8α+
D
CD103-
CD8α+
CD11b+
E
CD172a
CD8α
CD4
MHCII
CD40
Siglec F
F4/80
PDCA-1
CD80
CD86

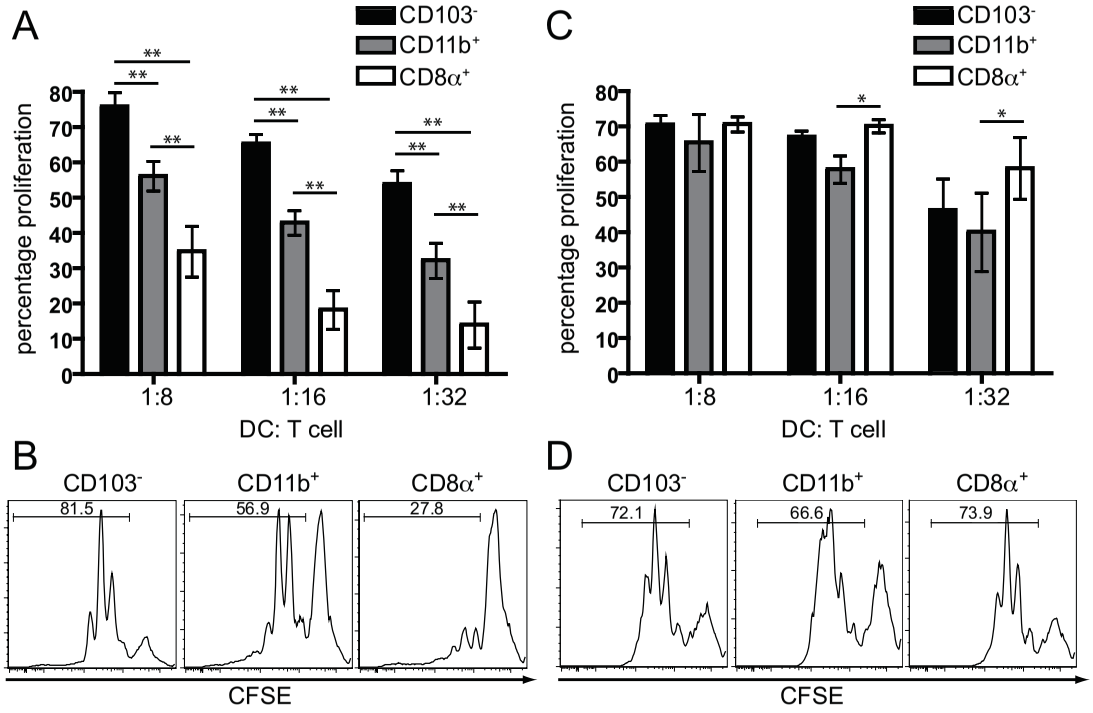
A
CD103-
CD11b+
CD8α+
percentage proliferation
80
70
60
50
40
30
20
10
0
**
1:8
1:16
1:32
DC: T cell
C
*
B
CD103-
CD11b+
CD8α+
81.5
56.9
27.8
CFSE
D
72.1
66.6
73.9

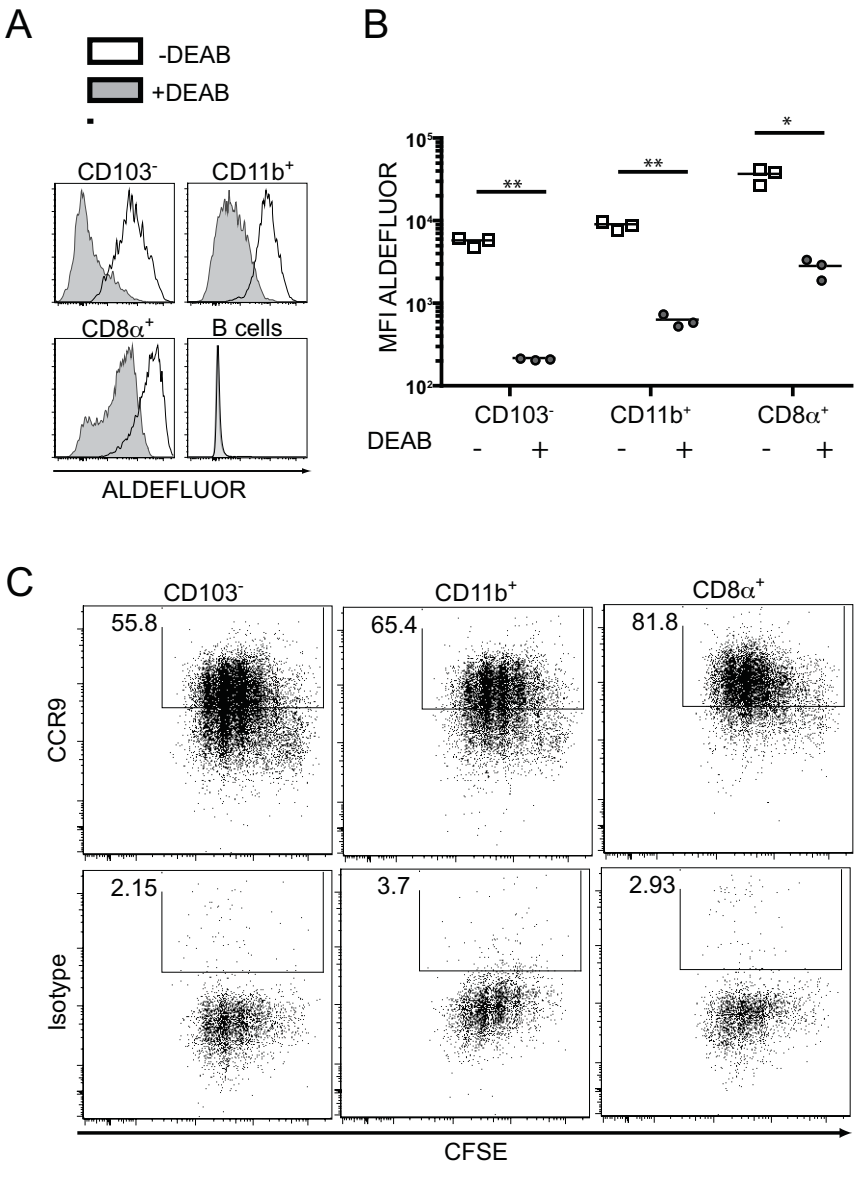
A
-DEAB
+DEAB
CD103-
CD11b+
CD8α+
B cells
ALDEFLUOR
B
MFI ALDEFLUOR
10⁵
10⁴
10³
10²
**
**
*
CD103-
CD11b+
CD8α+
DEAB
- + - + - +
C
CD103-
CD11b+
CD8α+
55.8
65.4
81.8
CCR9
2.15
3.7
2.93
Isotype
CFSE

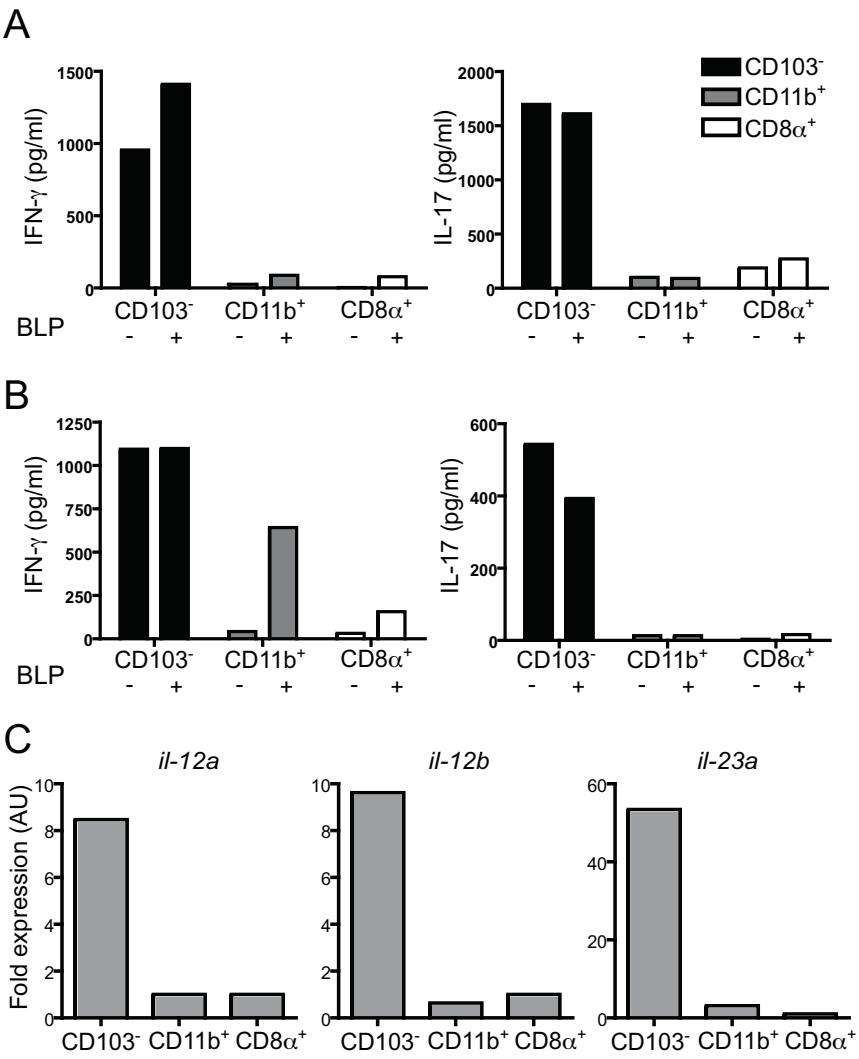
A
IFN-γ (pg/ml)
1500
1000
500
0
CD103-
CD11b+
CD8α+
BLP
- + - + - +
IL-17 (pg/ml)
2000
1500
1000
500
0
CD103-
CD11b+
CD8α+
B
IFN-γ (pg/ml)
1250
1000
750
500
250
0
CD103-
CD11b+
CD8α+
BLP
IL-17 (pg/ml)
600
400
200
0
C
il-12a
il-12b
il-23a
Fold expression (AU)
10
8
6
4
2
0
60
40
20
CD103- CD11b+ CD8α+

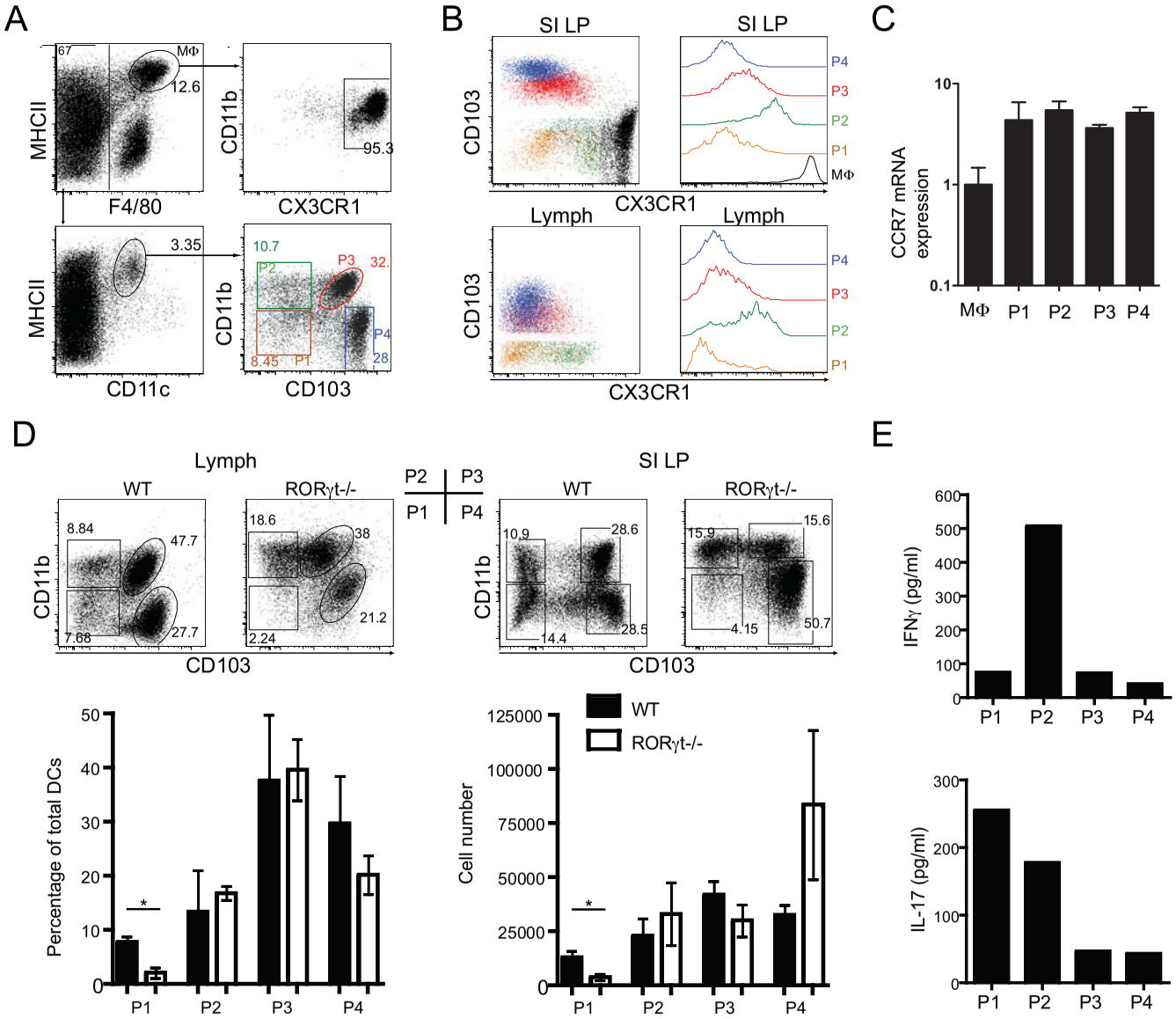
A
MHCII
F4/80
MΦ
12.6
CD11b
CX3CR1
95.3
MHCII
CD11c
3.35
CD11b
CD103
10.7
P2
P3
P4
P1
8.45
28
B
SI LP
SI LP
CD103
CX3CR1
P4
P3
P2
P1
MΦ
Lymph
Lymph
CD103
CX3CR1
C
CCR7 mRNA expression
10
1
0.1
MΦ P1 P2 P3 P4
D
Lymph
WT
RORγt-/-
P2 P3
P1 P4
SI LP
WT
RORγt-/-
CD11b
8.84
47.7
7.68
27.7
18.6
38
2.24
21.2
CD103
10.9
28.6
14.4
28.5
15.9
15.6
4.15
50.7
CD103
Percentage of total DCs
50
40
30
20
10
0
*
P1 P2 P3 P4
Cell number
125000
100000
75000
50000
25000
0
WT
RORγt-/-
*
P1 P2 P3 P4
E
IFNγ (pg/ml)
600
500
400
300
200
100
0
P1 P2 P3 P4
IL-17 (pg/ml)
300
200
100
0
P1 P2 P3 P4

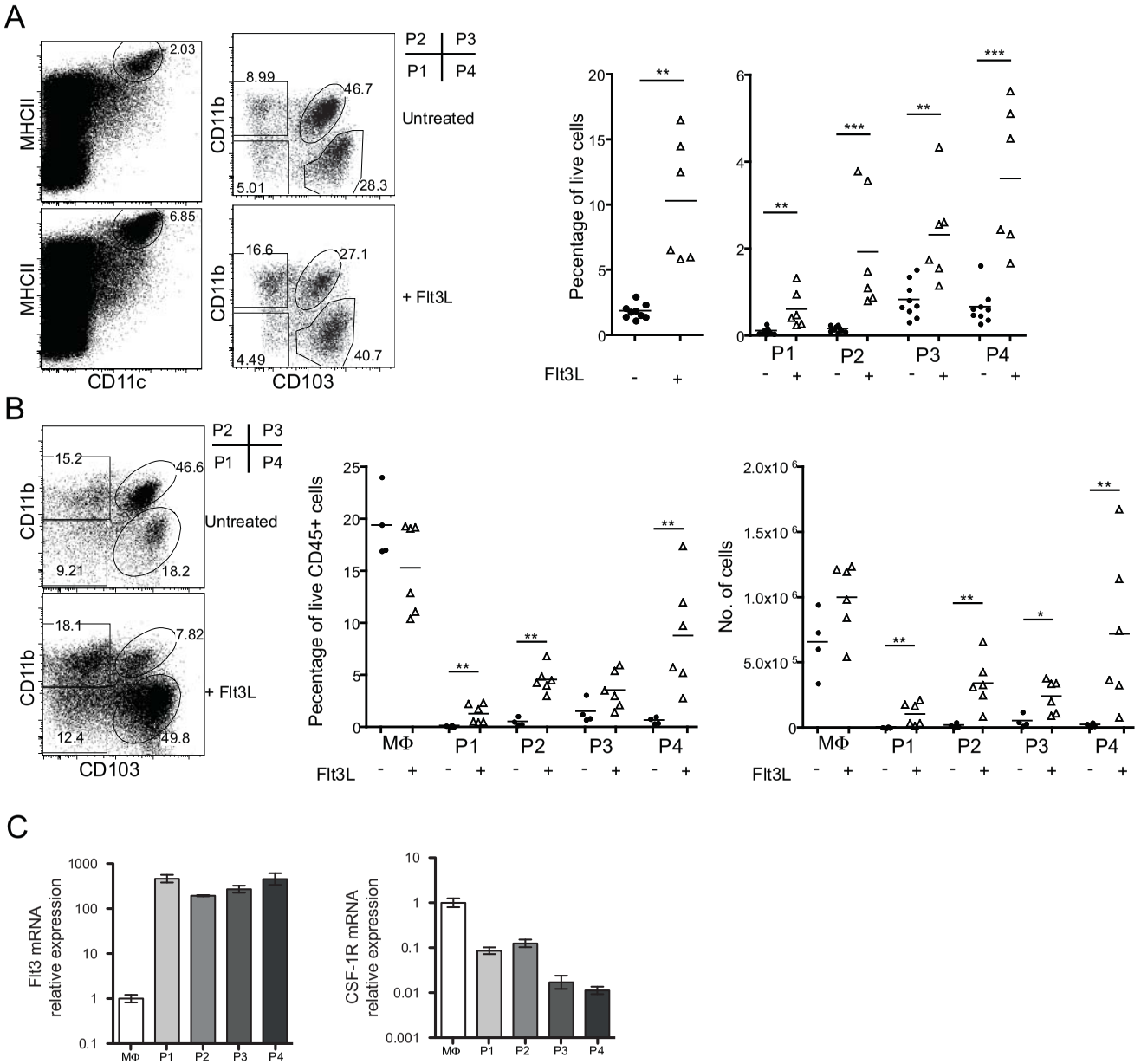
A
MHCII
CD11c
2.03
6.85
CD11b
CD103
8.99
46.7
5.01
28.3
16.6
27.1
4.49
40.7
P2
P3
P1
P4
Untreated
+ Flt3L
Pecentage of live cells
Flt3L
B
15.2
46.6
9.21
18.2
18.1
7.82
12.4
49.8
Pecentage of live CD45+ cells
No. of cells
MΦ
P1
P2
P3
P4
C
Flt3 mRNA relative expression
CSF-1R mRNA relative expression

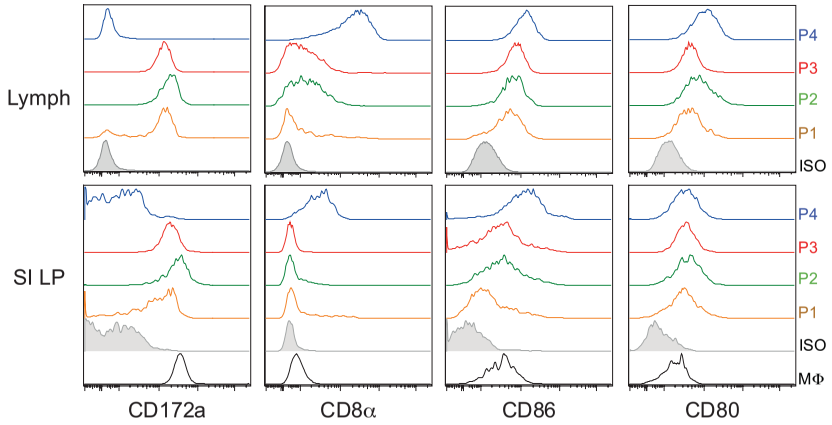
Lymph
SI LP
P4
P3
P2
P1
ISO
MΦ
CD172a
CD8α
CD86
CD80